Study of WW $\rightarrow q\bar{q}\ell\bar{\nu}$ at ILC500 with ILD

Justin Anguiano

(Dated: November 5, 2019)

An analysis of the semileptonic WW process used to benchmark ILD performance at center of mass energy 500 GeV, with an emphasis on the measurement of the W-boson mass and width.

I. INTRODUCTION AND MOTIVATION

II. PHYSICS

A. The Standard Model

The current standard model consists of two types of elementary particles: fermions and bosons. The fermions have a half-integer spin (1/2) and can be further separated into two categories: quarks and leptons. The quarks have three known generations, the first being the light quarks up(u) and down(d), the next generation gets increasingly more massive with the charm(c) and strange(s) quarks, and the most massive generation consists of the top(t) and bottom(b) quarks. Each individaul quark also carries a fractional electrical charge of either $+2/3$ for the uplike quarks (u,c,t) or $-1/3$ for the downlike quarks (d,s,b). The charged leptons are also comprised of three generations of increasing mass, they are the electron(e), muon(μ), and tau(τ). Each charged lepton is accompanied by neutrally charged neutrino ν_e, ν_μ, ν_τ. Bosons can be subdivided into two groups as well, the vector bosons and scalar boson. The singular scalar boson is the spin 0 Higgs Boson, responsible for giving particles mass. There are four known vector bosons the photon(γ), gluon(g), $W^\pm$, and Z^0. Each vector boson has a spin of 1 and each governs specific interactions between particles. The most well known boson is the photon, the photon mediates interaction between particles which have charge.The gluon mediates the strong force and is responsible for the interactions between quarks. The W and Z bosons are the mediators of the weak force and the only known particles that interact with neutrinos.

— *The W-boson*

The W boson is electrically charged where as its partner the Z is electrically neutral. The W boson decays through a flavor changing vertex, meaning that the particles involved in the decay vertex are always different flavors, and often the same generation, as long as charge and lepton number is conserved. Examples of the W fundamental vertices coupling with fermions is shown in Figure 1. The rate at which the W decays hadronically(to a pair of quarks) or Branching Ratio(BR) is $\approx 70\%$. The rate at which a charged lepton and neutrino is produced is $\approx 30\%$ and is split approximately evenly between the three charged leptons. The most difficult reconstruction of a final state from W decay is the case of a tau lepton. The tau can mimic the signature of hadrons or other leptons in a detector in addition to producing additional missing energy via neutrinos. The tau has a shorter lifetime compared to the other charged leptons and flies a short distance before decaying. If produced from the interaction point in a detector, the tau will travel on average $8\,\mu$m before decaying. The other leptons, like the electron, is stable and doesn't decay, and the muon is not stable but is unlikely to decay inside of the detector. The tau lepton mainly decays hadronically – into a tau neutrino and virtual W-boson that produces a pair of quarks. The virtual W's daughter quarks will hadronize into a charged particle ($\pi^\pm$) or radiate more quarks that form either more charged or neutral particles (π^0). If π^0's are created they immediately decay into two photons. When a tau produces a single charged particle this is classified as a 1-prong decay, 3 charged particles is classified as a 3-prong decay. The virtual W in the tau decay is allowed to decay into leptons, so, the tau final state can include either a electron or muon along with the corresponding flavor neutrinos. The decay rates for tau are given in Table I.

— *The W Mass*

The W-boson is an unstable particle and abides by a total decay rate $\Gamma = 1/\tau$ where τ is the average lifetime. A consequence of this decay length is that the observed mass distribution will approximately follow a Breit-Wigner distribution. The mass distribution is centered on the nominal W mass M_W with a width characterized by the full width half maximum Γ_W. The current highest precision measurement for the mass and width are results of measurements through W^+W^- production. These measurements use the combined results from LEP and Tevatron experiments which reports $M_W = 80.379 \pm 0.012$ GeV and $\Gamma_W = 2.085 \pm 0.042$ GeV [6]. The diagrams representing WW are given in Figure 2. The final states of the WW process are either the fully hadronic $WW \to q\bar{q}q\bar{q}$, semileptonic

	Decay Mode	Branching Ratio
Hadronic Modes (64.79%)	$\pi^-\nu_\tau$	10.82%
	$\pi^-\pi^0\nu_\tau$	25.49%
	$\pi^-\pi^0\pi^0\nu_\tau$	9.26%
	$\pi^-\pi^0\pi^0\pi^0\nu_\tau$	1.04%
	$\pi^-\pi^+\pi^-\nu_\tau$	8.99%
	$\pi^-\pi^+\pi^-\pi^0\nu_\tau$	2.74%
Leptonic Modes (35.21%)	$e^-\nu_e\nu_\tau$	17.82%
	$\mu^-\nu_\mu\nu_\tau$	17.39%

TABLE I. Most common decay modes for the τ^- lepton [6]

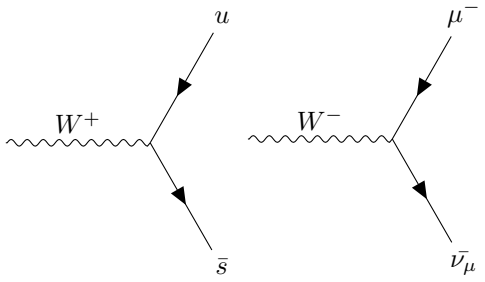

FIG. 1. Fundamental vertices between the W-boson and fermions

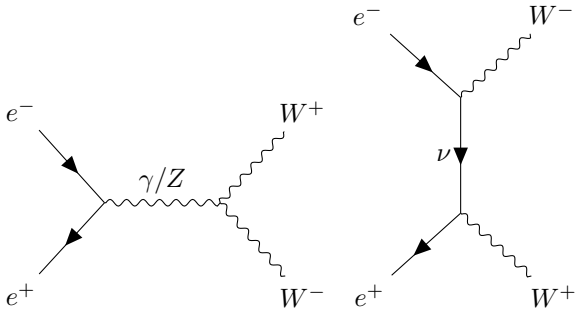

FIG. 2. WW processes

$WW \to q\bar{q}\ell\nu_\ell$, or fully leptonic $WW \to \ell\nu\ell\nu$. The semileptonic mode is the most favorable way to measure the W mass because the hadronic system is easily obtained after the identification of the lepton. The hadronic mode is more challenging due to the combinatoric assignment of the four hadronic jets into two W's. The leptonic channel is also difficult because of the presence of two neutrinos.

B. The Anatomy of an Event

— *Beam effects*

Figure 2 illustrates the production of WW through initial state $e^-\,e^+$ annihlation. Within the collider e^-e^+ annihilation presents two important effects. The first is beamstrasshlung or initial state radiation(ISR), this process occurs when one of the electron/positron beams radiates a photon. The radiated photon generally goes undetected by escaping down the beam-pipe causing the effective center of mass energy to be reduced at the interaction point. Secondary particles from ISR can also scatter into the detector and mix in with the event of interest. These ISR particles add a source of confusion wherein the foreign particles "pile-up" ontop of the true particles of an event, thus trying to resolve the true particles of the event becomes more challenging.

— *Helicity*

The second underlying physics property in every event is related to the helicity(spin) of the electron and positron. There are four possible combinations of electron positron helicities where each initial particle is either left or right handed. More explicitly, a collision can consist of $e^-_L e^+_R$(LR) with left handed electron and right handed positron , $e^-_R e^+_L$(RL) with right handed electron and left handed positron, or mirroring helicities RR and LL. The beams in the collider are mixed with multiple helicities which is represented by an overall partial beam polarizations P_{e^-} P_{e^+}. A diagram of possible tree-level spin configuration is shown in Figure II B. In the s-channel, the electron positron helicities are directly coupled, therefore, two W-bosons can only be produced in LR and RL configurations, whereas

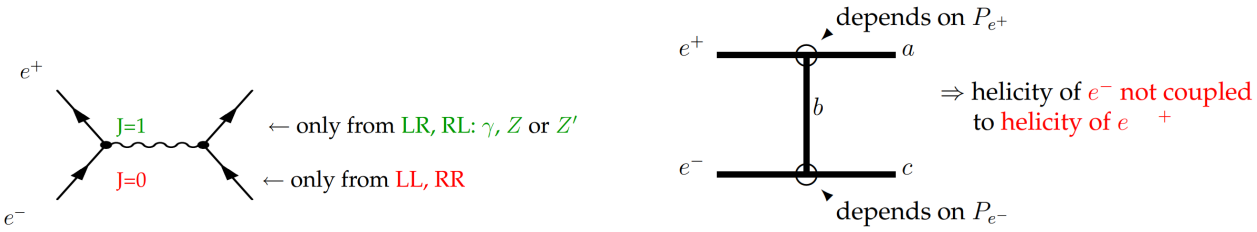

FIG. 3. Possible spin configurations in the s and t channel. [5]

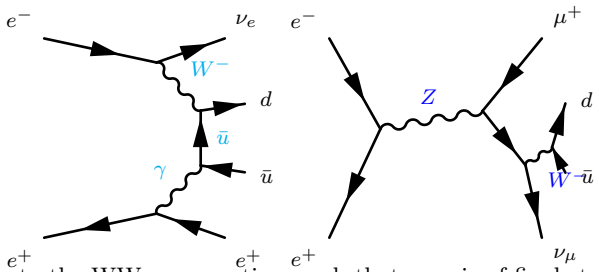

FIG. 4. Non signal-like contributions to the WW cross-section, such that, a pair of final state particles are not constrained to the W mass distribution.

in the mirrored configuration the recombination into particle of spin 1 is not possible. In the t-channel diagrams, the W's are directly coupled to the beam particles. The W has pure coupling only to left handed electrons or right handed positrons so the number of WW events produced are sensitive to the beam polarization. If the number of events produced is sensitive to polarization then the overall cross-section for WW production is sensitive to beam polarization.

— *Cross-section*

The cross-section is an important measurement because it verifies consistency with the underlying standard model predictions for the rate at which a process occurs. This measurement is doubly important for the WW process because it implicitly provides a in situ measurement of the beam polarizations. By definition, the cross-section is a cross-sectional area and represents the probability of an interaction. The total number of events N observed for a process is given by $N = \sigma L$ the cross-section is denoted by σ and L is the integrated luminosity which is a measure of the total number of collisions. In a physics analysis the desired process(signal) is accompanied other processes(background) that can unfortunately be nearly indistinguishable from the signal events. Topologocial or kinematic cuts are applied to each event to minimize the contamination of background events that enter the signal region when trying to count the number of signal events. This reduces the number of observed events N by the number of events lost to the event selection cuts. Thus the number of events observed is then

$$N = \sigma L \epsilon \tag{1}$$

where ϵ is the efficiency of the signal selection in Monte Carlo simulation. The signal efficiency is defined as:

$$\epsilon = \frac{\text{The number of signal events that pass selection}}{\text{The total number of signal events that can be selected}} \tag{2}$$

One thing to note is that for a specific process the cross-section includes contributions from all Feynman diagrams that have the same initial and final state particles. This includes diagrams that are essentially not "signal-like" for WW examples of these contribution diagrams are given in Figure 4.

III. THE ILC AND ILD

A. Accelerator Description

The search for new physics drives center of mass energies higher and higher. The current most powerful operating collider is the Large hadron collider, LHC at cern with center of mass energies of 13-14TeV. Since the dominating QCD background and busy environment that is created from many parton collision creates a significant challenge discoering new physics, the next frontier in high energy physics is naturally a linear accelrator(linac) through electron and positron collisions. This is because electron an positron are light particles they can not be accelerated to as high of energy as hadrons but are amenable to precision measurments because of the clean environment. The shape of the collider is also important because synchotron radiation is more with lighter particles but only if the particle changes direction. The last major electron positron collider was LEP which reached center of mass energies of around 200 GeV which still provides the dominating electroweak precision measurments that are good today. The ILC is next proposed future collider which would harness center of mass energies from 200GeV up to a possible 1 TeV upgrade. The proposed design was originally to start at 500 GeV center of mass energy along a 30km linac. Prohibitive costs have pushed the starting center of mass energy to 250 GeV with a 20 km linac with possible 500 GeV and 1 TeV upgrades as well as luminosity upgrades. The starting luminosity planned to be achieved is 1.35 1034 cm2s1, leading to a integrated luminosity of 2 ab1 after a decade. The acclerator will have an electron beam that polarised to 80%, and and positron source which will deliver a beam with a 30% positron polarisation.[1] A more detailed description of the accelrator designs can be found the Technical Design Report(TDR) [**?**].

B. Detector Description

There are two proposed detectors at the ILC which would serve the same interaction point on a push-pull mechanism. Where one detector will take data while the other is under maintenance. This allows for continuous collection of data, the opportunity for complimentary detector designs, offering the competition between detector experiments, and cross-checks between experimental results. All with the benefit of lower overall cost since there is only a single interaction point(IP). The two proposed detectors are the International Large Detector(ILD) and the Silicon Detector(SiD). Both detectors are shell components, outward from the interactions point is a vertex detector, tracker used to identify charged particles, a soleniod which produces the magnetic field bending incident charge particles. an electromagnetic calormiter which measures light particles and photons, a dense hadronic calorimter to stop and contain the showers from heavier particles. and a external muon layer which detects muons. The forward regions have a collection of calormiters designed to capture beam particles scattered at small angles. Both detectors optimize reconstruction of particles by the use of the Particle Flow Algorithm(PFA). PFA is method that that combines algorhitms and a highly granular calorimiter to fully resolve individual particles and their energy deposits [**?**]. ILD approach to PFA optimization is by making the detector large, thus physically separating the particle more making reconstruction easier. SiD approach is towards cost efficiency with a smaller detector and strong magnetic field to achieve a similar performance. The major difference between the two detector are the tracking mechanisms. The ILD is planned to use a gaseous central tracker with Time projection chamber. which provides a nearly continuous path information for tracks by providing up to 224 hits per track. SiD is planned to use a silicon tracking system similar to the LHC. The design demands for both detectors are as follows: at least 4μm spatial resolution in the vertex detector , momentum resolution $\Delta 1/p2^{-5}\,\mathrm{GeV}^{-}1$, a jet energy resolution 3%. and hermicity specifically to capture and conserve momentum from particles in the forward region in order to benefit analysis driven by missing energy.

C. Software

The software ecosystem for ILC is contained under ILCSOFT [**?**] which is comprised of reconstruction tools that rely on the event data model LCIO. FUll simulation samples generated are based on detector descriptions in DD4HEP [**?**] and physics samples centrally produced with Whizard [**?**]

IV. MEASUREMENT OF THE W MASS AND OTHER FEATURES

A. Lepton ID

The approach towards the identification of leptons is treat each flavor of lepton universally. A cone based approach is used capture narrow isolated jets that have low track multiplicity. The lepton acceptance criteria consists of these parameters:

- search cone angle - The opening (half) angle of the search cone for the lepton jet [rad]
- isolation cone angle - The outer isolation cone angle w.r.t to the search cone [rad]
- isolation energy - The total energy allowed within the isolation cone region [GeV]
- Invariant Mass The upper limit on the lepton candidate mass [GeV]
- pt seed - the minimum pt of a track that seeds a lepton candidate [GeV]

Additional requirements are imposed on all of the reconstructed PFOs in the event in order to suppress pile up particles being included in the lepton jet.

- pt > 0.2 GeV
- $|cos\theta| < 0.99$

The formation of a lepton follows three steps (1) candidate construction, (2) candidate merging, (3) isolation testing. The first step starts with a list of seed tracks sorted by energy in descending order. The track energy is calculated with respect to an assumed mass that is imposed by Pandora PFA. A track that qualifies as a seed track forms a new lepton candidate, any track that falls within the search cone of the lepton candidate is added to the lepton candidate, with each newly added particle the energy and momentum is updated for the lepton candidate. When a track has been added to a lepton candidate it is removed from the track seed list. Next, the neutral particles that fall inside the search cone are added to the lepton candidate. The neutral particles also reside on a list, and are removed from the list if added to a lepton candidate, this enforces uniqueness for each lepton candidate. Lepton candidates are continually formed until the list of seed tracks is completely exhausted. When there are no more candidates to be created, the candidates are subjected to the some of the acceptance criteria: the lepton jet mass is required to be below upper mass limit (2 GeV) and the number of charged tracks within the jet is non-zero and less than or equal to 4. If a lepton jet violates these conditions it is deleted. The next step in the process is merging. If two lepton candidates fall within each others search cones, the candidates are merged. If the mass or track multiplicity conditions are violated, both lepton candidates are deleted. All of the surviving candidates of the merging step are subjected to the isolation testing. For each candidate, the sum of energy of all the particles that fall inside the isolation cone is computed. If the total energy inside the isolation cone is greater than the maximum allowed energy inside the isolation cone the lepton candidate is deleted.

The acceptance criteria for leptons are optimized according to lepton flavor and τ decay topology. The categories created are:

- Prompt μ
- Prompt e
- $\tau \to \mu\bar{\nu_\mu}\nu_\tau$
- $\tau \to e\bar{\nu_e}\nu_\tau$
- $\tau \to$ hadrons (1-prong)
- $\tau \to$ hadrons (3-prong)

The Prompt categories refer to events which the leptonic W decays directly to either a muon or electron and associated neutrino. The tau categories address the various dominant decay topologies of the tau lepton. For each category we find the optimal lepton acceptance criteria where only the events that match the desired topology are considered for the category in question.

The optimal acceptance criteria is the set of parameters that most correctly identify lepton candidate jets that originate from true leptons while fail to fake lepton candidates that originate from hadronic jets. To find this set of parameters, a scan over a 3D space is performed using the search Cone-α, isolation cone-β, and isolation energy-E_{iso}. The invariant mass is held at a fixed 2 GeV for simplicity. The ranges and step sizes through this space are:

- $\alpha \in [0, 0.15]$ rad with 0.01 rad steps
- $\beta \in [0, 0.15]$ rad with 0.01 rad steps
- $E_{iso} \in [0, 5.5]$ GeV with 0.5 GeV steps

Two uncorrelated push-pull optimization parameters are defined to find the optimal working point in the lepton finding space. The first is related to correctly identifying jets originating from true leptons. This is denoted as the efficiency of reconstructing a true lepton ϵ_T. The second optimization parameter is denoted as P_F, the probability of a fake lepton jet arising from a single hadronic jet.

$$\epsilon_T = N_{match}/N_{Stotal} \tag{3}$$

$$\begin{aligned} P_F &= 1 - (1 - \epsilon_F)^{\frac{1}{4}} \\ \epsilon_F &= N_{fake}/N_{Btotal} \end{aligned} \tag{4}$$

The true lepton reconstruction efficiency is maximized with the signal sample $WW \to q\bar{q}\ell\bar{\nu}$. The denominator represents the total, category specific, number of events which contain three generator visible fermions($q\bar{q}\ell$ that all fall within the acceptance range $|cos\theta| < 0.99$. N_{match} is the number of signal sample events in which a lepton candidate jet is reconstructed and can be matched to the true lepton, such that the opening angle between the reconstructed lepton and the true lepton are less than 0.1 radians. The distribution of opening angles is shown if Figure X. In the case that a reconstructed lepton is being matched to a generator tau, the matching angle is between the reconstructed lepton and the vector formed from the sum of the visible generator components of the tau decay. The visible components of the tau decay consist of the direct decay products whereas photons from final state radiation are excluded. The fake lepton probability is minimized using the background sample $WW \to q\bar{q}q\bar{q}$ and is a function of the fake lepton reconstruction efficiency ϵ_F. The fake efficiency denominator is the total number of

events with visible generator fermions that fall within the same acceptance range $|cos\theta| < 0.99$. The numerator is the total number of events in which contain at least one reconstructed fake lepton. The 4-quark sample fake efficiency represents the binomial probability of r-successes(lepton reconstructions) in 4 trials(hadronic jets). The probability of a single success in a single trial, P_F, can be directly derived from the Binomial p.d.f using the fake efficiency ϵ_F. The optimal parameters α, β, E_{iso} for each lepton category are extracted from $\max[(1 - P_F)\epsilon_T]$. The results for each category are shown in Table X.

Since there is only one expected lepton jet in the signal sample, a single lepton jet is selected as the candidate for the event. If there are multiple lepton jets reconstructed in a single event the lepton jet with the highest energy is selected as the single candidate for the event. The Energy distribution of true and fake leptons is shown in Figure X. If the two highest energy lepton jets are of equal energy then the candidate selected will be the jet with the highest energy original seed track, based on the original seed track sorting. Any additional lepton jets that are not selected are treated as part of the hadronic system.

B. Pileup mitigation

Following the lepton selection the remaining particles in the system are expected to form the hadronically decaying W boson. However, the sum of the four momenta of the paricles produces a distrbution that is often greater than the true hadonic mass. Figure X shows the systematic mismeasurement of the hadronic W mass. Small variations between the true W mass and measured W mass naturally arise due to the mismeasurment of particles – specically neutral hadrons. If the diffence between the measured and true W mass is signifcantly negative it means that hadronic particles have been lost due to acceptance. Events in which the difference between the measured and true W mass is significantly positive indicates that the hadronic system contains particles that are not associated with the WW process i.e. pileup. To combat the measuerment excess due to pileup jet clustering algorithms via FastJet[2] are used. The standard approach for pileup mitigation is to use the kT algorithm[3] and tune the R parameter such that the pileup particles are associated with beam jets while the desired particles are associated to non beam jets. With successful kT clustering the beam jets can be thrown away without damaging the reconstruction of the desired event. However, this approach only works well in events that are centrally produced. The leading cross-section of WW in the $e^-_L e^+_R$ polarization yields an kinematic topology where the down like quark tends to be boosted forward causing overlap between the jet particles and pile-up particles. In this topology employing the kT algorithm leads to rejecting desired particles and severe undermeasuremnt of the the W mass. The solution to proper pileup mitigation is through jet fragmentation. Using the standard JADE algorithm which has no beam jet association and uses the mass based cutoff parameter $y_{cut} > y_{ij}$ where $y_{ij} = M^2_{ij}/Q^2$ with M_{ij} being the invariant mass of the pair of objects being combined and Q^2 being the visible energy in the e^+e^- annihilation [4]. By tuning the y_{cut} parameter the mass of individually reconstructed jets can be controlled. For large ycut values O(1e-3) a single massive jet is reconstructed and in the limit that ycut becomes infinitely small the number of jets reconstructed is the number of reconstructed particles. The ycut value chosen is the value that forms mini-jets that safely couple together hard and soft emissions from the original parton while segregating pile into its own mini-jets. The mini-jets are then subjected to kinematic cuts that are chosen to maximize the pileup rejection and minimize the rejection of true W daughter particles. The optimal ycut and mini-jet kinematic cut combination are selected over the range

- $y_{cut} \in [1 \times 10^{-3}, 0.5 \times 10^{-3}, \ldots, 4.5 \times 10^{-6}, 5 \times 10^{-6}$
- mini-jet $pT < x$ where $x \in [0, 5]$ in bins of 0.5 GeV
- mini-jet $|cos\theta| < y$ where $y \in [0.9, 1]$ in 0.01 bins

The optimization parameters used to select best combination are two statisical estimators from the distribution of $M_{qq}^{meas} - M_{qq}^{true}$. This binned mass difference distribution is created from the subset of mini-jets that arise from clustering with a given y_{cut} and and also pass some jet veto cut x and y. The estimators are the Full Width Half Maximum(FWHM) and the number of entries in the Mode. Using estimators calculated from a binned histogram creates unwanted sensitivity to bin size. To workaround this feature various tricks are employed. First the mode is defined as the center of the bin with the most entries the mode entries is the number of entries in the mode bin plus the number of entries in the mode bins nearest neighbors. For the FWHM, the mass distribution is assumed to be monotonically decreasing around the half maxmimum.

C. EventSelection

V. FUTURE ANALYSIS

VI. CONCLUSIONS

[1] et al Bambade, Philip.

[2] Gavin P. Salam Cacciari, Matteo and Gregory Soyez. Fastjet user manual.

[3] et al. Catani, Stefano. Longitudinally-invariant k-clustering algorithms for hadron-hadron collisions., 1993.

[4] et al Dokshitzer, Yu L. Better jet clustering algorithms., 1997.

[5] GA Moortgat-Pick, T Abe, G Alexander, B Ananthanarayan, A Babich, et al. The role of polarized positrons and electrons in revealing fundamental interactions at the linear collider, phys. rept. 460, 131–243 (2008). *arXiv preprint hep-ph/0507011*.

[6] M. Tanabashi, K. Hagiwara, K. Hikasa, K. Nakamura, Y. Sumino, F. Takahashi, J. Tanaka, K. Agashe, G. Aielli, C. Amsler, M. Antonelli, D. M. Asner, H. Baer, Sw. Banerjee, R. M. Barnett, T. Basaglia, C. W. Bauer, J. J. Beatty, V. I. Belousov, J. Beringer, S. Bethke, A. Bettini, H. Bichsel, O. Biebel, K. M. Black, E. Blucher, O. Buchmuller, V. Burkert, M. A. Bychkov, R. N. Cahn, M. Carena, A. Ceccucci, A. Cerri, D. Chakraborty, M.-C. Chen, R. S. Chivukula, G. Cowan, O. Dahl, G. D'Ambrosio, T. Damour, D. de Florian, A. de Gouvêa, T. DeGrand, P. de Jong, G. Dissertori, B. A. Dobrescu, M. D'Onofrio, M. Doser, M. Drees, H. K. Dreiner, D. A. Dwyer, P. Eerola, S. Eidelman, J. Ellis, J. Erler, V. V. Ezhela, W. Fetscher, B. D. Fields, R. Firestone, B. Foster, A. Freitas, H. Gallagher, L. Garren, H.-J. Gerber, G. Gerbier, T. Gershon, Y. Gershtein, T. Gherghetta, A. A. Godizov, M. Goodman, C. Grab, A. V. Gritsan, C. Grojean, D. E. Groom, M. Grünewald, A. Gurtu, T. Gutsche, H. E. Haber, C. Hanhart, S. Hashimoto, Y. Hayato, K. G. Hayes, A. Hebecker, S. Heinemeyer, B. Heltsley, J. J. Hernández-Rey, J. Hisano, A. Höcker, J. Holder, A. Holtkamp, T. Hyodo, K. D. Irwin, K. F. Johnson, M. Kado, M. Karliner, U. F. Katz, S. R. Klein, E. Klempt, R. V. Kowalewski, F. Krauss, M. Kreps, B. Krusche, Yu. V. Kuyanov, Y. Kwon, O. Lahav, J. Laiho, J. Lesgourgues, A. Liddle, Z. Ligeti, C.-J. Lin, C. Lippmann, T. M. Liss, L. Littenberg, K. S. Lugovsky, S. B. Lugovsky, A. Lusiani, Y. Makida, F. Maltoni, T. Mannel, A. V. Manohar, W. J. Marciano, A. D. Martin, A. Masoni, J. Matthews, U.-G. Meißner, D. Milstead, R. E. Mitchell, K. Mönig, P. Molaro, F. Moortgat, M. Moskovic, H. Murayama, M. Narain, P. Nason, S. Navas, M. Neubert, P. Nevski, Y. Nir, K. A. Olive, S. Pagan Griso, J. Parsons, C. Patrignani, J. A. Peacock, M. Pennington, S. T. Petcov, V. A. Petrov, E. Pianori, A. Piepke, A. Pomarol, A. Quadt, J. Rademacker, G. Raffelt, B. N. Ratcliff, P. Richardson, A. Ringwald, S. Roesler, S. Rolli, A. Romaniouk, L. J. Rosenberg, J. L. Rosner, G. Rybka, R. A. Ryutin, C. T. Sachrajda, Y. Sakai, G. P. Salam, S. Sarkar, F. Sauli, O. Schneider, K. Scholberg, A. J. Schwartz, D. Scott, V. Sharma, S. R. Sharpe, T. Shutt, M. Silari, T. Sjöstrand, P. Skands, T. Skwarnicki, J. G. Smith, G. F. Smoot, S. Spanier, H. Spieler, C. Spiering, A. Stahl, S. L. Stone, T. Sumiyoshi, M. J. Syphers, K. Terashi, J. Terning, U. Thoma, R. S. Thorne, L. Tiator, M. Titov, N. P. Tkachenko, N. A. Törnqvist, D. R. Tovey, G. Valencia, R. Van de Water, N. Varelas, G. Venanzoni, L. Verde, M. G. Vincter, P. Vogel, A. Vogt, S. P. Wakely, W. Walkowiak, C. W. Walter, D. Wands, D. R. Ward, M. O. Wascko, G. Weiglein, D. H. Weinberg, E. J. Weinberg, M. White, L. R. Wiencke, S. Willocq, C. G. Wohl, J. Womersley, C. L. Woody, R. L. Workman, W.-M. Yao, G. P. Zeller, O. V. Zenin, R.-Y. Zhu, S.-L. Zhu, F. Zimmermann, P. A. Zyla, J. Anderson, L. Fuller, V. S. Lugovsky, and P. Schaffner. Review of particle physics. *Phys. Rev. D*, 98:030001, Aug 2018.